Surface defects and conduction in polar oxide heterostructures

N. C. Bristowe,[1,2] P. B. Littlewood,[1] and Emilio Artacho[2,3]

[1] *Theory of Condensed Matter Group, Cavendish Laboratory, University of Cambridge, JJ Thomson Ave, Cambridge CB3 0HE, UK*

[2] *Department of Earth Sciences, University of Cambridge, Downing Street, Cambridge CB2 3EQ, UK*

[3] *Donostia International Physics Centre, Universidad del Pais Vasco, 20080 San Sebastian, Spain*

(Dated: March 28, 2011)

The polar interface between $LaAlO_3$ and $SrTiO_3$ has shown promise as a field effect transistor, with reduced (nanoscale) feature sizes and potentially added functionality over conventional semiconductor systems. However, the mobility of the interfacial two-dimensional electron gas (2DEG) is lower than desirable. Therefore to progress, the highly debated origin of the 2DEG must be understood. Here we present a case for surface redox reactions as the origin of the 2DEG, in particular surface O vacancies, using a model supported by first principles calculations that describes the redox formation. In agreement with recent spectroscopic and transport measurements, we predict a stabilization of such redox processes (and hence Ti 3*d* occupation) with film thickness beyond a critical value, which can be smaller than the critical thickness for 2D electronic conduction, since the surface defects generate trapping potentials that will affect the interface electron mobility. Several other recent experimental results, such as lack of core level broadening and shifts, find natural explanation. Pristine systems will likely require changed growth conditions or modified materials with a higher vacancy free energy.

I. INTRODUCTION

Complex oxides offer the potential to replace conventional semiconductors in a range of devices due to reduced feature sizes and added functionality (see e.g. ref.[1,2]). The polar interface between $LaAlO_3$ (LAO) and $SrTiO_3$ (STO) [3] has shown promise as a field effect transistor [4,5]. One problem hindering its development is the low mobility of the interface two-dimensional electron gas (2DEG). To progress, the origin of the 2DEG must be understood. Explanations proposed to date can be classed into three categories: (*i*) electron transfer countering the "polar catastrophe"[6], (*ii*) doping through O vacancies in the film[5,7–9] or in the substrate[10–12], and (*iii*) cation intermixing at the interface[6,13,14]. Growth conditions have been shown to affect the observed behavior, particularly O_2 partial pressure and post-annealing treatments, affecting carrier density and confinement to the interface (as opposed to conduction through the STO substrate)[4,11].

The polar catastrophe[6] arises from a polarization discontinuity between the non-polar STO substrate and polar LAO film [15]. In LAO films grown on TiO_2 terminated STO substrates this polar discontinuity induces a divergence of the electric displacement field ($\vec{\nabla} \cdot \vec{D}$) in the pristine system equal to considering the effective polarization response and net effective charges σ_c of precisely $+e/2$ and $-e/2$ per formula unit at the interface and surface, respectively[15–17]. The electrostatic potential then builds up across the LAO film, accumulating electrostatic energy. To counter it a charge transfer between the interface and the surface is required. A mechanism intrinsic to the pristine system is given by the transfer of electrons from the surface to the interface. From band bending arguments, electrons are transferred from the O 2*p* at the top of the valence band at the LAO surface, to the Ti 3*d* conduction band at the interface, once the potential drop across the LAO layer reaches the effective band gap, which is calculated to happen for a LAO thickness of five unit cells (see ref.[18] and within). However the absence of a 2D hole gas at the surface and the observation of populated Ti 3*d* states for films as thin as one or two bilayers[19–21] raises doubts about this mechanism.

Two important points should be kept in mind. Firstly, the samples are generally not kept or measured in vacuum. The surface can thus be covered by adsorbants like water, and it will likely be far from an ideal surface termination, possibly including chemical alterations such as the hydroxylation seen on many wet oxides. The second point is more central, however: whatever the chemistry, the relevant electrostatics across the film can only be affected by processes in which charge is altered at each side of the film, either by charge transport across it, or by charges arriving at either side from external reservoirs. If there are no such external sources and the chemical processes are confined to the surface, the remaining possibility is that of surface redox processes. They transform surface bound charge into free-carrier charge, the electrons or holes then being free to move to the buried interface. The clearest and quite relevant example is that of oxygen vacancy formation whereby surface O^{2-} anions transform into O_2 molecules, releasing two electrons to the *n* interface, as illustrated in Fig. 1[5,7–9]. Surface protonation[22,23] is an analogous process in which the surface is also reduced by the oxidation of O^{2-} into O_2, although in this case the process depends on the presence of water, $H_2O \rightarrow 1/2\ O_2 + 2e^- + 2H^+$, and both the energetics and kinetics will be different from the previous one[22]. The protons attach to the surface O atoms, while the electrons are again free to go to the *n* interface (note that the non-redox hydroxylation, $H_2O \rightarrow OH^- + H^+$, does not affect the electrostatics across the film).

In section II we present a model for the formation of surface redox processes. We then apply the model to the LAO/STO system in section III using parameters obtained from first-principles calculations (see appendix). We show that, for such a surface redox process, (*i*) the process is favored by film thickness through the effect of the electric field across the film; (*ii*) the growth of the density of the related surface defects with film thickness is predicted, showing a minimum critical thickness; (*iii*) the model is in excellent agreement with first principles calculations and reasonable agreement with what is observed experimentally for Ti 3*d* occupation; (*iv*) the potential drop across the film does not change substantially with thickness once vacancies start to appear; (*v*) for thin films the carriers at the interface are still trapped by the electrostatic potential generated by the vacancies in deep double-donor states: a strongly disordered two-dimensional electron system; (*vi*) as thickness increases the levels become shallower and the number density increases, closing the gap to the conduction band; (*vii*) the conduction onset is therefore at a higher film thickness than the one for interfacial carrier population. Finally we note that the model can also be applied to *p*-type interfaces and ultra thin ferroelectric films, where alteration of the surface chemistry has also been proposed as a possible screening mechanism (see for example ref.[24]).

II. MODEL

We consider a pristine polar thin film on a non-polar substrate defining a *n*-type interface (see Fig. 1), and a surface reduction process (the model can be trivially extended to *p*-type interfaces and surface oxidizing reactions, see below, and to ferroelectric thin films). The introduction of a surface defect via a redox reaction produces a donor level in the gap. The defect provides Z electrons (two for an O vacancy) that can transfer to the interface (see Fig. 1), thus contributing to the screening of the polarization or compositional charge σ_c at either side of the polar film ($\pm 0.5e$/f.u. in LAO [15–17]).

Considering this electron migration, we can model the formation energy of one such surface defect, E_f, in the presence of an area density n of surface defects as

$$E_f(n) = C + E_{\mathcal{E}}(n) + \alpha n, \tag{1}$$

where we have separated an electrostatic term associated with the internal electric field in the film, $E_{\mathcal{E}}(n)$, from a surface/interface chemistry term, C, and a term accounting for defect-defect interactions other than electrostatic in a mean-field sense. It can be seen as arising from

$$E_f(n) = E_f^0 - Z(W - E_{CD}) + E_{\mathcal{E}}(n) + \sum_i^{others} J_i r_i, \tag{2}$$

where E_f^0 is the formation energy of an isolated surface defect in the absence of a field across the film, and where

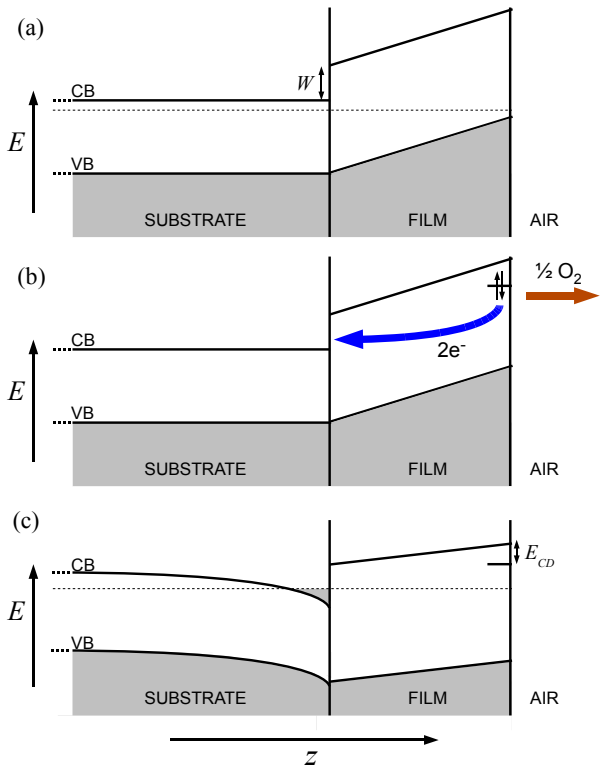

FIG. 1: (Color online) Schematic band diagram of an interface between a polar film and a non-polar substrate along the normal direction, z. (a) The pristine system under the critical film thickness. (b) The creation of a donor state at the surface via a redox reaction and subsequent electron transfer. (c) The reconstruction reduces the film's electric field.

W and E_{CD} are defined in Fig. 1[41]. E_f^0 (and thus C) depends on the particular surface chemical process, and the reference chemical potential for the relevant redox counterpart species in the environment, e.g. $\mu_{O_2}(P,T)$, which depends on experimental conditions.

Taking Eq. 1, the surface excess energy for a given area density of surface defects is then

$$\Omega(n) = \int_0^n E_f(n')\mathrm{d}n' = Cn + \Omega_{\mathcal{E}}(n) + \frac{1}{2}\alpha n^2. \tag{3}$$

The key of the proposed energy decomposition is that the $\Omega_{\mathcal{E}}$ term is simply the energy gain of partly discharging a capacitor, which is

$$\Omega_{\mathcal{E}}(n) = \frac{d}{2\epsilon}\left[(\sigma_c - \sigma_v)^2 - \sigma_c^2\right], \tag{4}$$

where d is the film thickness, ϵ is the LAO dielectric constant, σ_c is the compositional charge, and $\sigma_v = n(Ze)$ is the charge density of the carriers confined to the interface (note that these electrons may not all be mobile, as discussed below). Eq. 4 assumes no screening by electronic reconstruction, which is right if the onset for defect stabilisation happens earlier than the one for electronic reconstruction. A complete description of all possible regimes

will be presented elsewhere [25]. We limit ourselves to the regime given by Eq. 4 since a wider discussion of the model is irrelevant here.

The equilibrium defect density is determined by finding the value that minimizes Ω. Taking Eqs. 3 and 4,

$$n = \frac{d\,Ze\,\sigma_c - C\epsilon}{(Ze)^2 d + \alpha\epsilon}. \quad (5)$$

A critical thickness arises for defect stabilization,

$$d_c = C\epsilon/(Ze\sigma_c), \quad (6)$$

n tending to σ_c/Ze for large d, which is the value required to completely screen the film's intrinsic polarization.

III. DISCUSSION

A. Interface carrier density

We now consider the specific case of O vacancy formation at the surface as the most prominent candidate redox process[5,7,9]. Fig 2a) shows quantitative agreement between the model's $\bar{E}_f = \frac{1}{n}\Omega(n) = \frac{1}{n}\int_0^n E_f dn'$ and first principles calculations of the surface vacancy formation energies in ref.[7] on the full LAO/STO structure. $\bar{E}_f$ is the right magnitude to compare to first-principles results since it accounts for the energy difference between the system with a given concentration of surface defects (n) and the pristine system ($n = 0$), per surface defect, thus $\Omega(n)/n$. The physical constants used in the model were determined independently by separate DFT calculations (see appendix) and then compared to DFT results for films of varying thickness (Fig. 2a)). The predicted behavior of n (and σ_v) in LAO/STO is shown in Fig. 2b), where it is compared with Ti $3d$ occupation (both trapped and mobile) as measured with HAXPES[19]. Two bands are plotted, the colored one uses a range in C, the striped one a range in α and ϵ (see appendix). The bulk dielectric constant of LAO is about 24[26]. It may be substantially different for a strained ultra-thin film (see ref.[18] and within) and so the range $21 < \epsilon < 46$ has been considered.

The agreement in Fig. 2b) between model and experiment is only qualitative given the ambiguities in some of the magnitudes of key parameters defining the problem, most notably the chemical potential of O_2 in experimental conditions. Despite this, the model predicts a critical thickness for the appearance of carriers at the interface for a LAO film thickness below the five unit cells predicted by the purely electronic mechanism. Other qualitative features observed but not understood in this system also find a natural explanation (below).

B. Electric field in LAO: pinning of potential drop

The electrostatic potential drop across the LAO film is

$$V = (\sigma_c - \sigma_v)d/\epsilon. \quad (7)$$

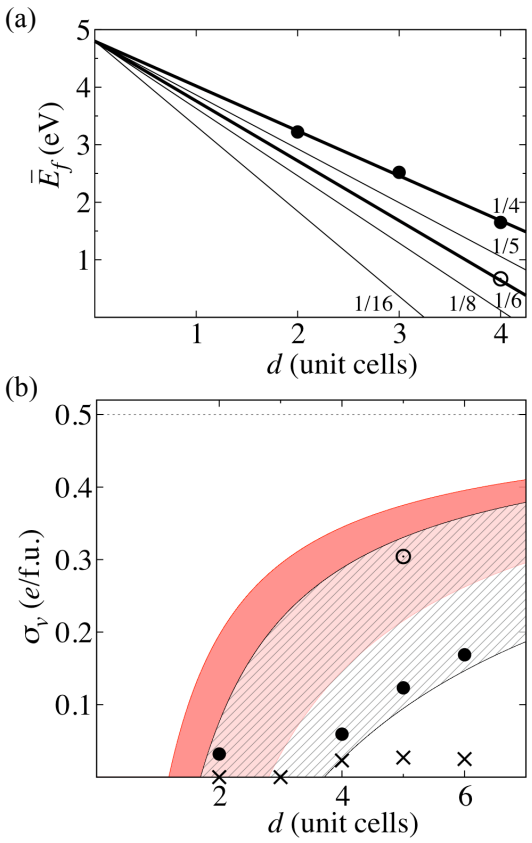

FIG. 2: (Color online) a) Defect formation energy, $\bar{E}_f$ (see definition in text) versus LAO film thickness d for various vacancy densities n. The model (lines) is compared with the DFT calculations (circles) of ref.[7] of the surface vacancy formation energy on the full LAO/STO structure (see appendix for the determination of the model parameters) b) Equilibrium area density of interface carriers σ_v versus d. The red (grey) band is the model prediction for 2.1 eV $< C <$ 5.0 eV, $\epsilon = 25$ and $\alpha = 0.8$ eV/(vac/f.u.)^2. The striped band is for $C = 3.6$ eV, $21 < \epsilon < 46$ and $0 < \alpha < 8$ eV/(vac/f.u.)^2. The circles indicate the Ti $3d$ occupation as measured with HAXPES in ref.[19]. Open circle indicates the sample was not annealed. The crosses indicate the carrier density from Hall measurements in ref.[4].

Substituting σ_v, the drop is essentially independent of thickness, $V \approx C/(Ze)$, when the vacancy-vacancy interaction is small, $\alpha \ll (Ze)^2 d/\epsilon$. Using the parameters for LAO/STO the difference in potential drop per LAO layer added is between 0.0 and 0.2 eV/f.u., much smaller than the predicted thickness dependence for the electronic screening model, and consistent with recent XPS measurements, which show no core level broadening with film thickness[27]. The pinning of V is also consistent with reduced cation-anion relative displacement with increasing LAO thickness as measured by SXRD[28].

C. Onset of conduction: electron trapping

The redox processes proposed above explain the absence of hole-mediated transport at the surface, while electrons allow 2D conduction at the interface. An important observation that remains unexplained, however, is the fact that the onset of interfacial Ti $3d$ occupation, as measured with HAXPES[19–21], happens at lower film thickness than the onset for interfacial 2D conduction[4]. It has been suggested that the 2DEG lies in several Ti $3d$ sub-bands, some of which are not mobile due to Anderson localization[29]. Whether Anderson localization occurs on an energy scale as high as room temperature depends on the energy scale of the disorder distribution. The surface defects associated to the redox processes represent point sources of effective charge, very much as a dopant in a semiconductor[17], e.g. $+2\ e$ for an O vacancy. They then generate trapping potentials for the carriers at the interface plane of the form $V_{\rm trap} = Ze^2/\epsilon\sqrt{\rho^2+d^2}$, in atomic units, where d is the film thickness and $\rho^2 = x^2 + y^2$ corresponds to the radial variable in the plane. This potential is sketched in Fig. 3 for several d values. Its depth decays with thickness as $1/d$. Fig. 3 shows estimates of the ground state electron level associated to the double donor state arising at the interface due to an O vacancy at the surface. These trapped interface levels may be the 'in-gap states' seen in a recent spectroscopic study[30]. For a thin film the traps are deep and few, but as it grows thicker, the donor states become shallower *and* the area density of traps grows, as illustrated in the inset of Fig. 3. A transition from insulating to conducting behavior is thus expected at a larger film thickness than the critical thickness for surface defect stabilization. With growing thickness, not only dopant levels tend to overlap as in a degenerate semiconductor, but the doping-level band is pushed towards the conduction band. For $Z = 2$, as for O vacancies, the physics of this transition is that of band overlap and disorder, since all dopant states are doubly occupied. If the mechanism involves $Z = 1$ defects, as in the hydroxylation case, the transition will be rather Mott-Anderson, as each dopant state is singly occupied. The different phenomenologies could be used to ascertain on the mechanism. The surface potential distribution from charged defects is consistent with a recent Kelvin probe force microscopy study[31].

IV. FINAL REMARKS AND CONCLUSIONS

A recent AFM study of LAO/STO has proposed the mechanism for conductivity switching[4,5] as the writing of surface charge[33]. Applying a biased tip to the surface alters the field across the LAO film which either increases or decreases the stability of vacancies (and hence σ_v) depending on the sign of the bias. An implication of this observation is that the kinetics for these redox processes is accessible at room T as used in these experiments, not only the much higher T used for growth.

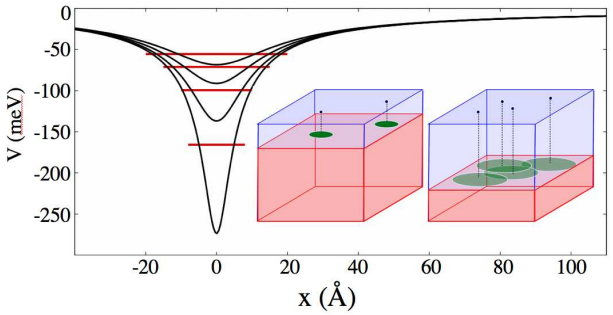

FIG. 3: (Color online) Trapping potential V created by a surface O vacancy as seen by interface electrons versus distance within the interface plane x (x=0 is directly below the vacancy) for film thickness $d = a$ (deepest), $2a, 3a, 4a$ (shallowest), with harmonic estimates of corresponding donor ground states (taking $m_{\rm eff} = 3{m_e}^{32}$). Inset: Sketch of range and density of trapped states.

The model proposed can also be used for p interfaces, holes, acceptor levels and surface oxidation processes. This would be the case for LAO grown on SrO terminated STO. It is less symmetric than it seems, however, since, in addition to different energetics and chemical potentials, the large conduction band offset at the interface (W in Fig. 1) favors the situation for electrons towards n interfaces much more than the much smaller valence band offset for holes and p-interfaces. For thin film ferroelectrics with outwards (inwards) polarization on metallic substrates, the important alignment becomes the acceptor (donor) level with the metal fermi level. This could be behind the stability of switchable ultra thin ferroelectric films under open circuit conditions (see e.g. ref.[24,34]).

We conclude that in LAO/STO, the onset of electrostatic modulation doping is precluded by the thermodynamic creation of surface defects and thus carrier mobilities produced by this method will be much lower than at a pristine interface. Intrinsic systems will likely require changed growth conditions or modified materials with a higher vacancy free energy.

Acknowledgments

We acknowledge H Hwang, M Pruneda and M Stengel for valuable discussions, the support of EPSRC and the computing resources of CamGRID at Cambridge University and the Spanish Supercomputer Network (RES).

Appendix: Model parameters

Here we describe the determination of the parameters, α, ϵ and C used in the model in Fig. 2 of the main paper. The parameters used in the model were independently determined from first principles in appropriate LAO-based systems (see below), and then the model was

checked against DFT calculations of vacancy formation energies in the full LAO/STO system as a function of thickness (Fig. 2a)). When comparing the model with experiment (Fig. 2b)), we account for inaccuracies of DFT and the ambiguity of the experimental chemical potential in the determination of each of these parameters.

1. The vacancy-vacancy interaction term, α

The defect-defect term was defined in Eq. 1 to include interactions other than electrostatic. Therefore to determine α we performed first principles calculations (see ref[16] for the method) of the charge neutral defect, i.e. oxygen vacancies in 'bulk' LAO which include the double donor electrons. One oxygen vacancy was placed in a simulation cell of 1×1×8, 2×2×8 and 3×3×8 unit cells of LAO to approximate 2D arrays of vacancies of various area densities. From the difference in formation energy per vacancy between the three calculations, α was found to be 0.8 eV/(vac/f.u.)^2, which was used in Fig 2a). α is formally defined as the interaction between vacancies at the film surface, however we believe this bulk value to be a good estimate. For the comparison with experiment, to account for any error associated with this determination we choose the range $0 < \alpha < 8$ eV/(vac/f.u.)^2 in Fig. 2b) of the paper.

2. The dielectric constant, ϵ

The dielectric constant, ϵ, consists of lattice and electronic contributions. For LAO, we take ϵ=28 as the total for Fig 2a), as consistent with ref.[35]. When comparing with experiment, we note the error and inconstancy of DFT calculations of ϵ, and additionally the effect of strain as highlighted in ref.[18]. Due to this we choose the range $21 < \epsilon < 46$ for Fig 2b).

3. The surface/interface chemistry term, C

C consists of three terms,

$$C = E^0_{f,\mu=0} + \mu + 2(E_{CV} - W) \qquad \text{(A.1)}$$

From the electronic structure presented by Li *et al.*, the last term is found to be approx. -1.2 eV. From first principles calculations of ref.[36] the formation energy of an isolated oxygen vacancy at the surface of LAO (in the absence of a field) with reference to oxygen in an isolated molecule ($1/2E[O_2]$), $E^0_{f,\mu=0}$, is approx. 6.0 eV. We define the zero of chemical potential relative to this reference state, which is appropriate for the DFT comparison and hence the value of C used in Fig. 2a) is taken as 4.8 eV.

The DFT underestimation of the band gap requires corrections to both $E^0_{f,\mu=0}$ (see ref.[37]) and W for the comparison with experiment in Fig. 2b). At this point we note the difficulties and variation in first principles determination of formation energies of donor/acceptor states (see for example ref.[38]).

From ref.[37], the formation energy correction of a donor defect, required due to DFT band gap underestimation is simply:

$$\Delta E^0_f = Z\Delta E_c \qquad \text{(A.2)}$$

where ΔE_c is the change in conduction band edge between LDA and experiment (or corrected DFT). By comparing the electronic structure presented in Li *et al.* and ref.[39], this correction could be as large as 1.0 eV. Therefore we take 6.0 eV $< E^0_{f,\mu=0} <$ 7.0 eV.

From experimental band alignment[40] and theoretical calculations determining the gap states[39], the third term in Eq. (A.1) is approx. 2.0 eV (not 1.2 eV). Correcting for these DFT errors we take,

$$4.0 \text{ eV} + \mu < C < 5.0 \text{ eV} + \mu \qquad \text{(A.3)}$$

The chemical potential of oxygen in the growth conditions used in ref.[19] (T = 1073 K and $p = 2.0 \times 10^{-8}$ atm) relative to the zero reference defined above is calculated to be -1.9 eV assuming the environment acts as an ideal gas-like reservoir. The effect of post-annealing and cooling to room temperature and pressure is to shift the chemical potential towards zero. With these limits on the chemical potential and the inequality in Eq. (A.3), the range of C becomes 2.1 eV $< C <$ 5.0 eV, as used in Fig. 2b).

[1] J. Mannhart and D. Schlom, Science **327**, 1607 (2010).
[2] H. Takagi and H. Hwang, Science **327**, 1601 (2010).
[3] A. Ohtomo and H. Hwang, Nature **427**, 423 (2004).
[4] S. Thiel, G. Hammerl, A. Schmehl, C. W. Schneider, and J. Mannhart, Science **313**, 1942 (2006).
[5] C. Cen, S. Thiel, G. Hammerl, C. W. Schneider, K. E. Andersen, C. S. Hellberg, J. Mannhart, and J. Levy, Nat. Mater. **7**, 298 (2008).
[6] N. Nakagawa, H. Hwang, and D. Muller, Nat. Mater. **5**, 204 (2006).
[7] Y. Li, S. Phattalung, S. Limpijumnong, and J. Yu, Arxiv preprint arXiv:0912.4805 (2009).
[8] Z. Zhong, P. Xu, and P. Kelly, Phys. Rev. B **82**, 165127 (2010).
[9] L. Zhang, X. Zhou, H. Wang, J. Xu, J. Li, E. Wang, and S. Wei, Phys. Rev. B **82**, 125412 (2010).
[10] G. Herranz, M. Basletic, M. Bibes, C. Carretero, E. Tafra, E. Jacquet, K. Bouzehouane, C. Deranlot, A. Hamzic, J.-

M. Broto, A. Barthelemy, and A. Fert, Phys. Rev. Lett. **98** (2007).
[11] W. Siemons, G. Koster, H. Yamamoto, W. A. Harrison, G. Lucovsky, T. H. Geballe, D. H. A. Blank, and M. R. Beasley, Phys. Rev. Lett. **98** (2007).
[12] A. Kalabukhov, R. Gunnarsson, J. Borjesson, E. Olsson, T. Claeson, and D. Winkler, Phys. Rev. B **75** (2007).
[13] P. R. Willmott, S. A. Pauli, R. Herger, C. M. Schlepuetz, D. Martoccia, B. D. Patterson, B. Delley, R. Clarke, D. Kumah, C. Cionca, and Y. Yacoby, Phys. Rev. Lett. **99** (2007).
[14] L. Qiao, T. Droubay, V. Shutthanandan, Z. Zhu, P. Sushko, and S. Chambers, J. Phys.: Condens. Matter **22**, 312201 (2010).
[15] M. Stengel and D. Vanderbilt, Phys. Rev. B **80**, 241103 (2009).
[16] N. C. Bristowe, E. Artacho, and P. B. Littlewood, Phys. Rev. B **80**, 45425 (2009).
[17] N. Bristowe, P. Littlewood, and E. Artacho, J. Phys.: Condens. Matter **23**, 081001 (2011).
[18] H. Chen, A. M. Kolpak, and S. Ismail-Beigi, Advanced Materials **22**, 2881 (2010).
[19] M. Sing, G. Berner, K. Goß, A. Müller, A. Ruff, A. Wetscherek, S. Thiel, J. Mannhart, S. Pauli, C. Schneider, P. R. Willmott, M. Gorgoi, F. Schafers, and R. Claessen, Phys. Rev. Lett. **102**, 176805 (2009).
[20] A. Fujimori, private communication .
[21] G. Berner, S. Glawion, J. Walde, F. Pfaff, H. Hollmark, L. Duda, S. Paetel, C. Richter, J. Mannhart, M. Sing, and R. Claessen, Phys. Rev. B **82**, 241405 (2010).
[22] W. J. Son, E. Cho, J. Lee, and S. Han, J. Phys.: Condens. Matter **22**, 315501 (2010).
[23] R. Anez, A. Sierraalta, G. Martorell, and P. Sautet, Surf. Sci. **603**, 25262531 (2009).
[24] R. Wang, D. Fong, F. Jiang, M. Highland, P. Fuoss, C. Thompson, A. Kolpak, J. Eastman, S. Streiffer, A. Rappe, and G. Stephenson, Phys. Rev. Lett. **102**, 47601 (2009).
[25] N. C. Bristowe, P. B. Littlewood, and E. Artacho, to be published (2011).
[26] J. Krupka, R. Geyer, M. Kuhn, and J. Hinken, IEEE Trans. Microwave Theory Tech. **42**, 2418 (1994).
[27] Y. Segal, J. Ngai, J. Reiner, F. Walker, and C. Ahn, Phys. Rev. B **80**, 241107 (2009).
[28] S. A. Pauli, S. J. Leake, B. Delley, M. Björck, C. W. Schneider, C. M. Schlepütz, D. Martoccia, S. Paetel, J. Mannhart, and P. R. Willmott, Phys. Rev. Lett. **106**, 036101 (2011).
[29] Z. S. Popovic, S. Satpathy, and R. M. Martin, Phys. Rev. Lett. **101**, 256801 (2008).
[30] G. Drera, F. Banfi, F. Canova, P. Borghetti, L. Sangaletti, F. Bondino, E. Magnano, J. Huijben, M. Huijben, G. Rijnders, D. Blank, H. Hilgenkamp, and A. Brinkman, Appl. Phys. Lett. **98**, 2907 (2011).
[31] V. Popok, A. Kalabukhov, R. Gunnarsson, S. Lemeshko, T. Claeson, and D. Winkler, Journal of Advanced Microscopy Research **5**, 26 (2010).
[32] A. Dubroka, M. Rössle, K. Kim, V. Malik, L. Schultz, S. Thiel, C. Schneider, J. Mannhart, G. Herranz, O. Copie, M. Bibes, A. Barthélémy, and C. Bernhard, Phys. Rev. Lett. **104**, 156807 (2010).
[33] Y. Xie, C. Bell, T. Yajima, Y. Hikita, and H. Hwang, Nano Lett. , 930 (2010).
[34] V. Garcia, S. Fusil, K. Bouzehouane, S. Enouz-Vedrenne, N. Mathur, A. Barthélémy, and M. Bibes, Nature **460**, 81 (2009).
[35] P. Delugas, V. Fiorentini, and A. Filippetti, Phys. Rev. B **71**, 134302 (2005).
[36] T. Jin-Long, Z. Jun, Q. Wen-Feng, X. Jie, and L. Yan-Rong, Chinese Physics B **17**, 655 (2008).
[37] C. Persson, Y. Zhao, S. Lany, and A. Zunger, Phys. Rev. B **72**, 35211 (2005).
[38] P. Deák, B. Aradi, T. Frauenheim, and A. Gali, Materials Science and Engineering: B **154**, 187 (2008).
[39] K. Xiong, J. Robertson, and S. Clark, Microelectron. Eng. **85**, 65 (2008).
[40] K. Yoshimatsu, R. Yasuhara, H. Kumigashira, and M. Oshima, Phys. Rev. Lett. **101** (2008).
[41] A valence band offset has been omitted for clarity since it is known to be small, but can also be included alongside the conduction band offset without affecting the model